LUPINE PUBLISHERS

Modern Approaches on Material Science

DOI: 10.32474/MAMS.2023.05.000208

ISSN: 2641-6921

Research Article

The Google Net-Assisted Phase Transition Detectors for Superconductors

Wong CH[1,2]*, Raymond PH[4], Wu H[5], Lei X[3] and Zatsepin AF[3]

[1]*Department of Industrial and Systems Engineering, The Hong Kong Polytechnic University, Hong Kong, China*

[2]*Research Institute for Advanced Manufacturing (RIAM) Engineering, The Hong Kong Polytechnic University, Hong Kong, China*

[3]*Institute of Physics and Technology, Ural Federal University, Yekaterinburg, Russia*

[4]*Department of Physics, The Chinese University of Hong Kong, Hong Kong, China*

[5]*State Key Laboratory of Catalysis, Dalian Institute of Chemical Physics, Chinese Academy of Sciences, Dalian, China*

***Corresponding author:** Wong CH, Department of Industrial and Systems Engineering, The Hong Kong Polytechnic University, Hong Kong, China

Received: April 12, 2023 **Published:** May 10, 2023

Abstract

For the superconductors suffering from phase fluctuations, finite electrical resistance exists below the pairing temperature Tc unless it undergoes Berezinskii-Kosterlitz-Thouless (BKT) transition where vortices and anti-vortices form pairs a particular temperature TBKT. As the distribution of vortices carries valuable information to understand the vortex-melting in superconductors, the Tc and TBKT must be identified in heavily overlapped heat capacity anomalies. To avoid misjudging T_{BKT}, we test whether or not the Google Net model can separate the overlapped anomalies without losing the primary information about the phase transitions, and test if it predicts the T_c and T_{BKT} in a new system accurately. Our work opens a path for the Google Net model to enter the world of superconductivity as an artificial-intelligence tool.

Keywords: Superconductors; Deep learning; Monte Carlo simulations

Introduction

To vanish the electrical resistance of superconductors, the phase and amplitude of the superconducting parameters must be ordered [1,2]. The phase fluctuations in low-dimensional superconductors and high-temperature bulk superconductors suppress the formation of a long-range ordered state even if the temperature is below the T_c [2-15]. The phase stability can be achieved by undergoing the Berezinski–Kosterlitz–Thouless (BKT) transition [3-5] at a lower critical temperature T_{BKT}, where a quasi-long range superconducting order is created. Despite the van Hove singularities [6] in the electronic density of states of 1D superconductors would be advantageous to produce a high T_c phenomenon, the superconducting phase slips at the 1D limit suppressing a long-range order at any finite temperature associated with a finite electrical resistance [7-11]. However, the disappearance of the phase fluctuations has been observed in the quasi-1D superconducting nanowires array under a transverse Josephson coupling J where a long-range-ordered superconducting state with zero resistance at finite temperature is obtainable [12-19].

In recent years, scientists aim at raising the T_{BKT} closer to the T_c [12,14] through understanding the mechanism of vortex-antivortex pairing. The critical temperatures for the system with multiple

phase transitions can be determined by searching the peaks of the heat capacity anomalies [4]. By inputting the experimental parameters (e.g., lattice parameters, electron concentration ...etc) into the XY model, the BKT transition and superconducting phase transition [4-20] can be generated where the degree of overlap is comparable to the experimental observations [11-20]. By plotting the distribution of phase vortices in the XY model, it unmasks the mechanism of vortex melting in different superconductors. However, in high-temperature bulk superconductors like Nb_3Sn, the heat capacity anomalies at the T_c and the T_{BKT} are heavily overlapped where the difference between these two-phase transition temperatures is ~0.2K only. When the experimental parameter of the Nb_3Sn superconductor is imported to the XY model, the almost completely overlapped anomalies in the XY model makes it difficult to identify the value of T_{BKT} accurately [15] even if advanced curve-fitting techniques are applied. If the distribution of phase vortices is misjudged at the wrong BKT transition temperature, it impedes the search for the mechanism behind the superconducting vortex-antivortex pairing. To solve this issue, a phase transition detector without showing overlapping phase transitions on the temperature domain is needed. The Google Net designed by the research teams at Google with the collaboration of several universities has been a forefront computer vision algorithm since 2014. [21] The Google Net model contains 1×1 convolutions in the middle of the architecture and global average pooling that establishes a deeper architecture of 22 layers deep with low computational cost [22,23]. Before we study the significantly overlapped transitions in the Nb_3Sn superconductors [15] we test whether the Google Net-assisted phase transition detector can separate the moderately overlapped transitions in the parallel 1D superconducting nanowires laterally coupled by Josephson interaction J as a preliminary investigation.

Method

The Monte Carlo method with the Metropolis algorithm is used to simulate the standard 8-state XY model (q = 8) on a square lattice, where the Josephson interaction J is spatial independent along the sample surface [4,7,12]. The phase maps as a series of temperature at equilibrium state are obtained. Then the phase maps are converted into the JPEG format for image classification. To identify the T_c at which two electrons form a Cooper pair (CP) [7] two thousand phase-maps with the size of 66 x 66 are simulated at the dimensionless T_c under the condition of average $J = |J_{sc} \sin(\delta\Theta)| = 1$, which is named the "stock data (CP)". The J_{sc} is the magnitude of Josephson energy and $\delta\Theta$ refers to the phase difference during the tunneling process. To locate the T_{BKT} at which the vortex and anti-vortex form a pair [4,20], two thousand phase-maps with the size of 66 x 66 are generated at the dimensionless T_{BKT} under the condition of J = 1, which is named as the "stock data (BKT)". Then we create the "test data (q = 8, J = 1)" and the "test data (q = 8, J = 0.8)" where two thousand 66 x 66 phase-maps are generated at each temperature, respectively. The image classification is based on the GoogLeNet model under the Convolutional Neural Network (CNN) [21,22]. The image database is split into training data (70%) and validation data (30%). If the Google Net model can recognize the phase maps accurately, the validation accuracy of phase maps is close to 100%. To check whether the sample is located at the phase transition temperatures or not, the likelihood of the phase transitions, i.e. LH factor (CP) and LH factor (BKT), are defined as (100% - validation accuracy) / 50%. When the LH factor closes to 1, the material is expected to undergo the phase transition.

Results and Discussions

Figure 1 shows the thermal fluctuations which are generated by the 8-state XY model with J = 1 and J = 0.8. After a careful curve-fitting process, we get the $T_{BKT} = 0.34$ and the $T_c = 1.13$ for J = 1 in Figure 1a. Similarly, we get the $T_{BKT} = 0.32$ and the $T_c = 0.85$ for J = 0.8 in Figure 1b. This verifies that the values of T_{BKT} and T_c depend on the Josephson interaction J. The two thousand phase-maps simulated in the conditions of J = 1 and $T_c = 1.13$ are grouped as the "stock data (CP)". Meanwhile, the two thousand phase maps in the "stock data (BKT)" are created in the conditions of J = 1 and $T_{BKT} = 0.34$. The phase maps are plotted in Figure 2, respectively. The direction of phase is displayed in terms of a color-plot which is advantageous to image classification. In the 8-state XY model, the direction of superconducting phase at 0, 45, 90, 135, 180, 225, 270, 315 degrees refers to the integer 0, 1, 2, 3, 4, 5, 6, 7 in the color bar, respectively. Figure 1: Alt Text [21 words]: The black lines are the heat capacity data. The red curve is the smoothed data. Two heat capacity anomalies are observed. Figure 2 Alt Text: Four figures are shown. The distribution of grid color is more chaotic in the ascending order of (2a) < (2b) < (2c) < (2d) [21 words] According to Figure 3, the Google Net-assisted phase transition detector distinguishes the T_c and the T_{BKT} on the same domain very clearly. Although the traditional method [4] in Figure 1a shows that the BKT transition occurs at the $T_{BKT} \sim 0.3$, Figure 3a shows that the LH factor (CP) remains zero for T < 0.5. Zero LH factor (BKT or CP) means that undergoing the phase transition is not possible. For J = 1, the Google Net-assisted phase transition detector shows that the T_c is 1.1 with the evidence of the LH factor (CP) = 1. On the other hand, by replacing the "stock data (CP)" with the "stock data (BKT)" emerges the BKT transition at $T_{BKT} \sim 0.3$ as shown in Figure 3b, where the LH factor (BKT) = 1. The LH factor (BKT) returns to zero for T > 0.6 even though the superconducting phase transition occurs at $T_c \sim 1$. As the stock data and the test data in Figure 3 are computed by setting the J = 1 in the XY model [4] we proceed to examine the accuracy of the Google Net-assisted phase transition detector if the Josephson interaction in the stock data and the test data are not identical. Figure 4 demonstrates that the Google Net model [21,22] is capable of learning the features from the phase-maps in the J = 1 system and then interpreting the unknown phase transition temperatures in the 'unseen' systems ($J \neq 1$).

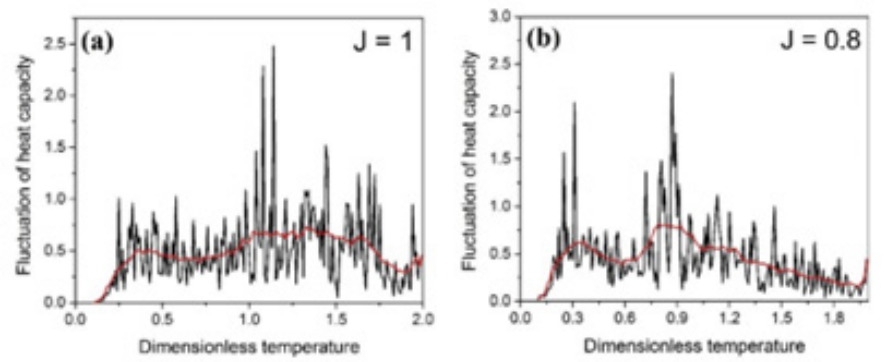

Figure 1: The fluctuations of heat capacity as a function of temperature (a) J = 1. (b) J = 0.8.

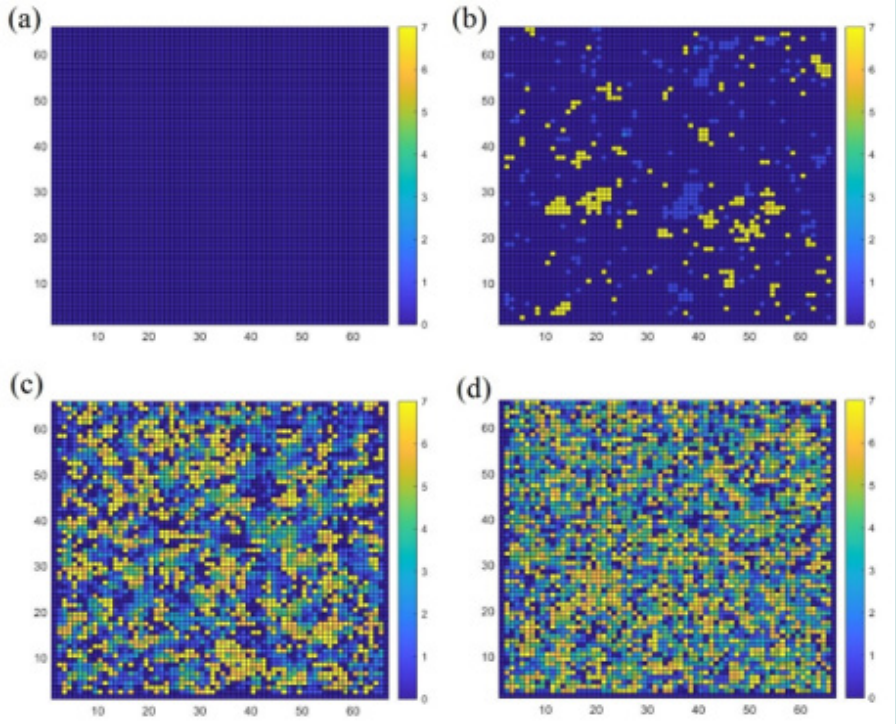

Figure 2: The phase-maps for J = 1 at different temperatures. (a) The phase-map below the T_{BKT}. (b) The phase-map at the T_{BKT}. (c) The phase-map at the T_c. (d) The phase-map above the Tc.

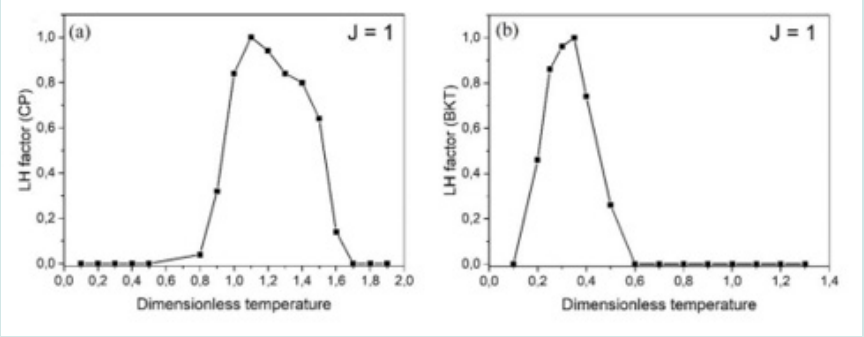

Figure 3: The LH factors as a function of temperatures. The stock data (CP), the stock data (BKT) and the test data are run by assigning the J = 1 in the XY model (a) The LH factor (CP) refers to the likelihood of forming the superconducting phase transition. (b) The LH factor (BKT) refers to the likelihood of undergoing the BKT transition.

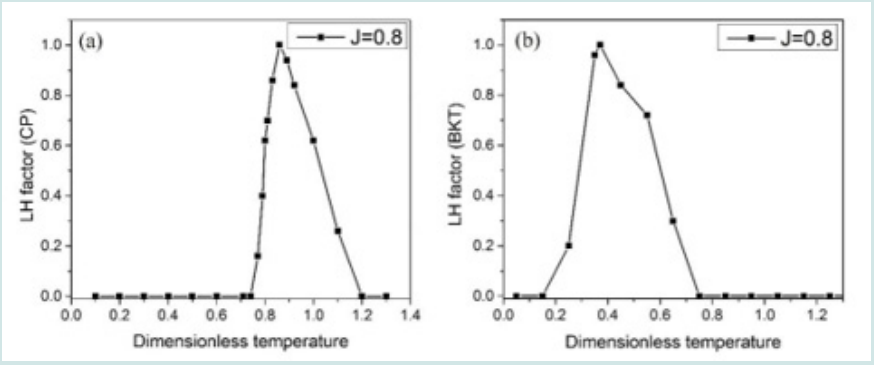

Figure 4: The LH factors as a series of temperatures. The stock data (CP), the stock data (BKT) are run by assigning the J = 1 in the XY model. The test data are prepared by setting the J = 0.8 in the XY model. (a) The LH factor (CP) of 1 corresponds to the superconducting phase transition temperature. (b) The LH factor (BKT) of 1 refers to the BKT transition temperature.

The prediction of the Google Net model in the J = 0.8 system is also accurate. Although Figure 1b illustrates the BKT transition at T ~ 0.3, Figure 4 confirms that the GoogLeNet-assisted phase transition detector can distinguish the T_c and the T_{BKT} effectively without overlapping. After the J is reduced to 0.8 in the "test data", Figure 4a shows that the LH factor (CP) is the highest at T_c = 0.83 where the superconducting phase transition takes place. No BKT transition is observed in Figure 4a. Again, in Figure 4b, changing the "stock data (CP)" to the "stock data (BKT)" emerges the BKT transition at T ~ 0.3 and the superconducting phase transition at T ~ 1 is disappeared. The LH factor (BKT) becomes zero for T > 0.7 in Figure 4b. Figure 3: Alt Text: (3a) A peak of the bump is located at ~T=1. (3b) A peak of the bump is located at ~T=0.4. [20 words] Figure 4: Alt Text: (4a) A peak of the bump is located at ~T=0.9. (4b) A peak of the bump is located at ~T=0.4 [20 words]. When we draw a parallel between Figure 1, Figure 3 and Figure 4, the phase transition temperatures probed by the GoogLeNet model [21,22] are almost identical to the traditional method of heat capacity measurement [4,12,20]. However, there is a big advantage of using the GoogLeNet-assisted phase transition detector: the superconducting phase transition and the BKT transition can be observed separately. If the traditional method is used to probe the phase transition temperature [4] these two heat capacity anomalies emerge on the same temperature domain in Figure 1, which requires advanced numerical methods [12-15] to distinguish the T_{BKT} and the T_c. Without the advanced curve fitting techniques, one may argue that there are three heat capacity anomalies at T ~ 0.3, T ~ 1 and T ~ 1.7 in Figure 1a. After we fit the curves carefully with help of the scientific knowledge and numerical mathematics [12-15] we can figure out that the peaks at T ~ 1.7 do not refer to the superconducting phase transition temperature. In contrast, probing the superconducting transition temperature via the use of the LH factor can avoid this problem because the non-zero LH factor (CP) and LH factor (BKT) do not appear at the same temperature. Let us recall that a higher validation accuracy of the phase maps produces a lower LH factor. When the temperature is near the T_c or the T_{BKT}, the phase-maps in the "stock data" and the "test data" look similar. Then it reduces the validation accuracy and raises the LH factor where we make use of this trend to locate the phase transition temperatures. The GoogLeNet-assisted phase transition detector is accurate as shown in Figure 3. It is reasonable because the Josephson interactions in the "stock data" and the "test data" are the same. As the GoogLeNet model has learnt the features from the stock data at J =1, it interprets the phase map in the 'unseen' system (J = 0.8) successfully, because the distribution of phases at the T_c (or T_{BKT}) shares the same nature regardless of the value of J. We used a FUJITSU computer equipped with Intel(R) Core (TM) i7-3632QM CPU at 2.2GHz to train the phase transition detector that requires 25 minutes only. With this reasonable computational cost, it is possible to predict the phase transitions by using the artificial intelligence assisted XY model. As the Google Net-assisted XY model shows great success in separating the moderately overlapped phase transition, it gives hope to distinguish the T_c and the T_{BKT} in a heavily overlapped transition such as Nb_3Sn superconductors and is possibly applicable to other superconductors suffering from the same issue.

Competing Interests

The author(s) declare no competing interests.

Acknowledgements

We appreciate the Research Institute for Advanced Manufacturing and the Industrial Centre at The Hong Kong Polytechnic University to support this project. This research project was sponsored by (University Grants Committee – The Hong Kong Polytechnic University) with grant number (1-45-37-BD5C).

Availability of data

Data available on request from the authors

References

1. Hohenberg PC (1967) Existence of long-range order in one- and two-dimensions Phys Rev 158: 383-386.
2. Mermin ND, Wagner H (1966) Absence of ferromagnetism or anti ferromagnetism in one- or two-dimensional isotropic Heisenberg models. Phys. Rev Lett 17: 1133-1136.

3. Kosterlitz JM, Thouless DJ (1973) Ordering, metastability and phase transitions in two-dimensional systems. J Phys C 6: 1181-1203.
4. Kosterlitz JM (1973) The critical properties of the two-dimensional by model J Phys C 7: 1046-1060.
5. Berezinskii VL (1973) Destruction of long-range order in one-dimensional and two-dimensional systems having a continuous symmetry group I Classical system Sov Phys JETP 32: 493-500.
6. Van Hove L (1953) The occurrence of singularities in the elastic frequency distribution of a crystal Phys Rev 89: 1189-1193.
7. Tian M (2005) Dissipation in quasi-one-dimensional superconducting single-crystal Sn nanowires. Phys Rev B 71: 104521-104527.
8. Tian M (2003) Synthesis and characterization of superconducting single-crystal Sn nanowires. App Phys Lett 83: 1620-1622.
9. Yi G, Schwarzacher W (1999) Single crystal superconductor nanowires by electrode- position. Appl Phys Lett 74: 1746-1748.
10. Dubois S, Michel A, Eymery JP, Duvail JL (1999) Fabrication and properties of arrays of superconducting nanowires. J Mater Res 14: 665- 671.
11. Michotte S (2002) Superconducting properties of lead nanowires arrays. Physica C 377: 267-276.
12. He M (2013) Giant enhancement of the upper critical field and fluctuations above the bulk Tc in superconducting ultrathin lead nanowire arrays. ACS Nano 7: 4187-4193.
13. Bergk B (2011) Superconducting transitions of intrinsic arrays of weakly coupled one-dimensional superconducting chains: the case of the extreme quasi-1D superconductor Tl2 Mo6Se 6 New J Phys 13.
14. Wang Z (2010) Superconducting resistive transition in coupled arrays of 4Å carbon nanotubes. Phys Rev B 81: 174530-174539.
15. Lortz F, Lin N, Musolino Y, Wang A, Junod B, et al. (2006) Thermal fluctuations and vortex melting in the Nb3Sn superconductor from high resolution specific heat measurement, Phys Rev B 74: 104-502.
16. Stoeckly B, Scalapino DJ (1975) Statistical mechanics of ginzburg-landau fields for weakly coupled chains. Phys Rev B 11: 205-210.
17. Scalapino DJ, Imry Y, Pincus P (1975) Generalized Ginzburg-Landau theory of pseudo-one-dimensional systems. Phys Rev B 11: 2042–2048.
18. Schulz HJ, Bourbonnais C (1983) Quantum fluctuations in quasi-one-dimensional superconductors. Phys Rev B 27: 5856–5859.
19. Efetov KB, Larkin AI (1975) Effect of fluctuations on the transition temperature in quasi-one-dimensional superconductors. Sov Phys JETP 41: 76-79.
20. Wong CH, Wu RPH, Lortz R (2017) Phase fluctuations in two coaxial quasi-one-dimensional superconducting cylindrical surfaces serving as a model system for superconducting nanowire bundles. Physica C 45-49.
21. Tang PJ, Wang HK, Wong S (2017) G-MS2F: Google Net based multi-stage feature fusion of deep CNN for scene recognition. Neurocomputing 225: 188-197.
22. Hyeon-Joong (2015) Deep Convolution Neural Networks in Computer Vision: a Review, Trans. Smart Process. Comput. 4: 35-43.
23. Joaquin F, Rodriguez-Nieva, Mathias S (2019) Identifying topological order through unsupervised machine learning, Nature Physics 15: 790-795.

DOI: 10.32474/MAMS.2023.05.000208